Cell Metabolism
Article

Lysosome-Related Organelles in Intestinal Cells Are a Zinc Storage Site in *C. elegans*

Hyun Cheol Roh,[1] Sara Collier,[1] James Guthrie,[2] J. David Robertson,[2,3] and Kerry Kornfeld[1,*]
[1]Department of Developmental Biology, Washington University School of Medicine, St. Louis, MO 63110, USA
[2]Research Reactor Center
[3]Department of Chemistry
University of Missouri, Columbia, MO 65211, USA
*Correspondence: kornfeld@wustl.edu
DOI 10.1016/j.cmet.2011.12.003

SUMMARY

Zinc is an essential trace element involved in many biological processes and human diseases. Because zinc deficiency and excess are deleterious, animals require homeostatic mechanisms to maintain zinc levels in response to dietary fluctuations. Here, we demonstrate that lysosome-related organelles in intestinal cells of *C. elegans,* called gut granules, function as the major site of zinc storage. Zinc storage in gut granules promotes detoxification and subsequent mobilization, linking cellular and organismal zinc metabolism. The cation diffusion facilitator protein CDF-2 plays a critical role in this process by transporting zinc into gut granules. In response to high dietary zinc, gut granules displayed structural changes characterized by a bilobed morphology with asymmetric distributions of zinc and molecular markers. We defined a genetic pathway that mediates the formation of bilobed morphology. These findings elucidate mechanisms of zinc storage, detoxification, and mobilization in *C. elegans* and may be relevant to other animals.

INTRODUCTION

Zinc is a nutrient that is essential for all life. Zinc has roles in many biological processes; protein-bound zinc contributes to enzymatic activity and protein structure, and labile zinc functions in signal transduction (Murakami and Hirano, 2008; Vallee and Falchuk, 1993). Zinc is important for human health, since zinc deficiency causes a broad range of defects in multiple organ systems including skin, immune, skeletal, and reproductive (Hambidge, 2000). Zinc deficiency is associated with genetic diseases caused by mutations of zinc transporters, such as acrodermatitis enteropathica and inadequate dietary intake, which is a major world-wide problem. Excess zinc is also deleterious, since it may displace other trace metals or bind low affinity sites, leading to protein dysfunction (Fosmire, 1990). Therefore, organisms require homeostatic mechanisms to control the levels and distribution of this essential metal.

Zinc metabolism in animals is regulated at the organismal and cellular levels. In vertebrates, the gastrointestinal tract mediates zinc absorption, and absorbed zinc is distributed by the circulatory system (King, 2011). The gastrointestinal tract also plays a major role in zinc excretion, with smaller contributions from other tissues, including the kidney and pancreas. At the cellular level, zinc is partitioned between the cytoplasm and the lumen of intracellular organelles, and it can be labile or protein bound (Eide, 2006). Two families of zinc transporters play critical roles in these processes: cation diffusion facilitator (CDF/ZnT/SLC30) and Zrt-like, Irt-like protein (ZIP/SLC39) (Cragg et al., 2005; Feeney et al., 2005). CDF proteins decrease cytoplasmic levels by transporting zinc across the plasma membrane or into intracellular organelles, whereas ZIP proteins increase cytoplasmic levels by transporting zinc in the opposite direction. Mammals contain 10 CDF and 14 ZIP proteins that have specific tissue distributions and intracellular localizations (Lichten and Cousins, 2009). Thus, a network of zinc transporters is important for zinc metabolism in animals.

Mechanisms of zinc storage and mobilization have been characterized in the yeast *Saccharomyces cerevisiae* (Eide, 2009). When zinc is abundant, excess zinc is stored in the vacuole by the CDF proteins Cot1 and Zrc1. In response to zinc deficiency, the ZIP protein Zrt3 mobilizes stored zinc. Zinc accumulation has been demonstrated in mammalian cells. In response to high levels of zinc in the culture media, labile zinc accumulates in endosomal or lysosomal organelles, termed zincosomes (Haase and Beyersmann, 1999; Palmiter et al., 1996). In higher animals such as birds, a high zinc diet causes organismal zinc accumulation and promotes resistance to a subsequent dietary zinc deficiency (Emmert and Baker, 1995). Humans appear to have only a limited capacity for zinc storage and mobilization, since symptoms of zinc deficiency develop rapidly in response to dietary deficiency (King, 2011). An important question is how zinc storage at the cellular level contributes to the response to zinc deficiency at the organismal level in animals.

The nematode *C. elegans* is a useful model organism for the study of metal biology, including iron and heme metabolism, metal toxicity, and zinc signaling (Bruinsma et al., 2002; Gourley et al., 2003; Liao and Freedman, 1998; Rajagopal et al., 2008; Vatamaniuk et al., 2001; Yoder et al., 2004). To study zinc metabolism, we developed methods to manipulate dietary zinc and used forward and reverse genetic approaches to identify genes important for zinc metabolism (Bruinsma et al., 2008;

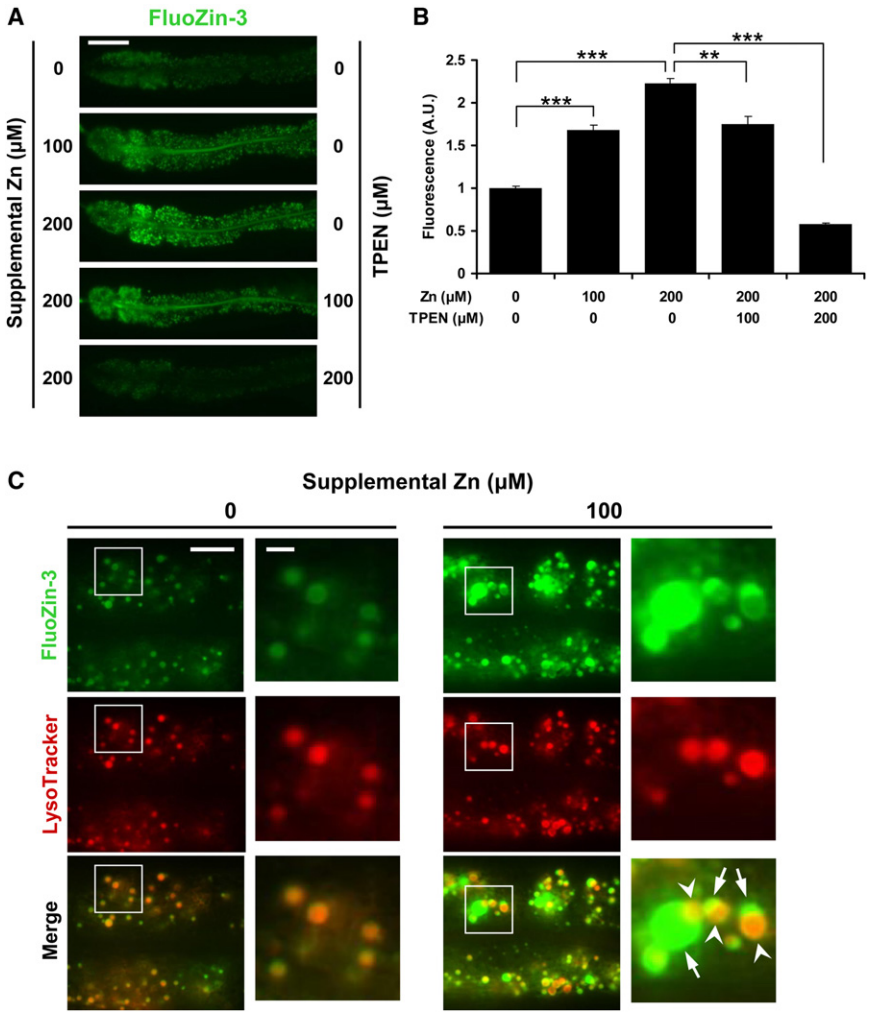

Figure 1. Zinc Is Stored in Gut Granules

(A) Fluorescence images of live wild-type hermaphrodites cultured with FluoZin-3 and the indicated levels of supplemental zinc and TPEN. Panels display the anterior half of the intestine of a single animal with pharynx to the left and tail to the right. Scale bar: 50 μm.

(B) Quantification of fluorescence images like those shown in (A) using ImageJ software. The fluorescence intensity (shown in arbitrary units, A.U.) was normalized by setting the value at 0 μM supplemental Zn equal to 1.0. Bars indicate mean values ± SEM (n = 15) (**p < 0.001; ***p < 0.0001).

(C) Fluorescence images of live wild-type animals costained with FluoZin-3 (green) and LysoTracker (red). Boxed regions are magnified in the right panels. Animals cultured with 100 μM supplemental zinc displayed bilobed gut granules with asymmetric staining; one side was strongly positive for FluoZin-3 (arrow), and the other side was strongly positive for LysoTracker (arrowhead). Scale bars: 10 μm and 2 μm (boxed regions) (see also Figures S1 and S2).

Davis et al., 2009; Murphy et al., 2011). *C. elegans* contains highly conserved families of CDF, ZIP, and metallothionein genes, suggesting that fundamental mechanisms of zinc metabolism may be similar to other animals. In response to a high zinc diet, *C. elegans* accumulates zinc (Davis et al., 2009). To characterize zinc storage and mobilization, we developed methods to visualize zinc in *C. elegans* using a zinc-specific fluorescent dye. We determined that zinc is stored in lysosome-related organelles in intestinal cells, and these organelles undergo a transition to a bilobed morphology in response to high dietary zinc. We demonstrated that zinc accumulation in these organelles, which is mediated by the activity of the CDF-2 zinc transporter, plays a critical role in zinc detoxification and mobilization in the physiological setting of an intact animal.

RESULTS

Gut Granules Contain Labile Zinc

By using inductively coupled plasma-mass spectrometry (ICP-MS) to measure total zinc content in worm extracts, we demonstrated that *C. elegans* cultured with high dietary zinc display elevated levels of total zinc, suggesting excess zinc is stored (Davis et al., 2009). To identify the site of zinc storage, we used zinc-specific fluorescent dyes to visualize zinc. We conducted pilot studies with several dyes and selected FluoZin-3 based on its high zinc sensitivity and specificity (Gee et al., 2002). Hermaphrodites were cultured on noble agar minimal medium (NAMM) dishes (Bruinsma et al., 2008) containing FluoZin-3, and live animals were analyzed by fluorescence microscopy. Wild-type animals cultured without supplemental zinc displayed green fluorescence in vesicles in intestinal cells (Figure 1A). FluoZin-3 fluorescence intensity displayed significant, dose-dependent enhancement and diminishment in worms cultured with supplemental zinc and the zinc chelator, N,N,N′,N′-tetrakis (2-pyridylmethyl) ethylenediamine (TPEN), respectively (Figures 1A and 1B). These results indicate that FluoZin-3 monitors labile zinc in live worms, and zinc is concentrated in vesicles of intestinal cells.

Gut granules in intestinal cells have been classified as lysosome-related organelles based on the presence of lysosomal proteins and staining with lysosome-specific fluorescent dyes such as LysoTracker (Clokey and Jacobson, 1986; Hermann et al., 2005; Kostich et al., 2000). To investigate the relationship between FluoZin-3 fluorescent vesicles and gut granules, we performed costaining experiments using LysoTracker. With no supplemental zinc, the patterns of FluoZin-3 and LysoTracker fluorescence were highly overlapping in intestinal cells (Figures 1C and S1), indicating that zinc detected by FluoZin-3 is stored in gut granules. Because gut granules contain birefringent and autofluorescent materials, we determined how autofluorescence compares to FluoZin-3 fluorescence by comparing control animals cultured with no dye to animals cultured with FluoZin-3. Animals cultured with FluoZin-3 displayed 2.6-fold, 3.5-fold,

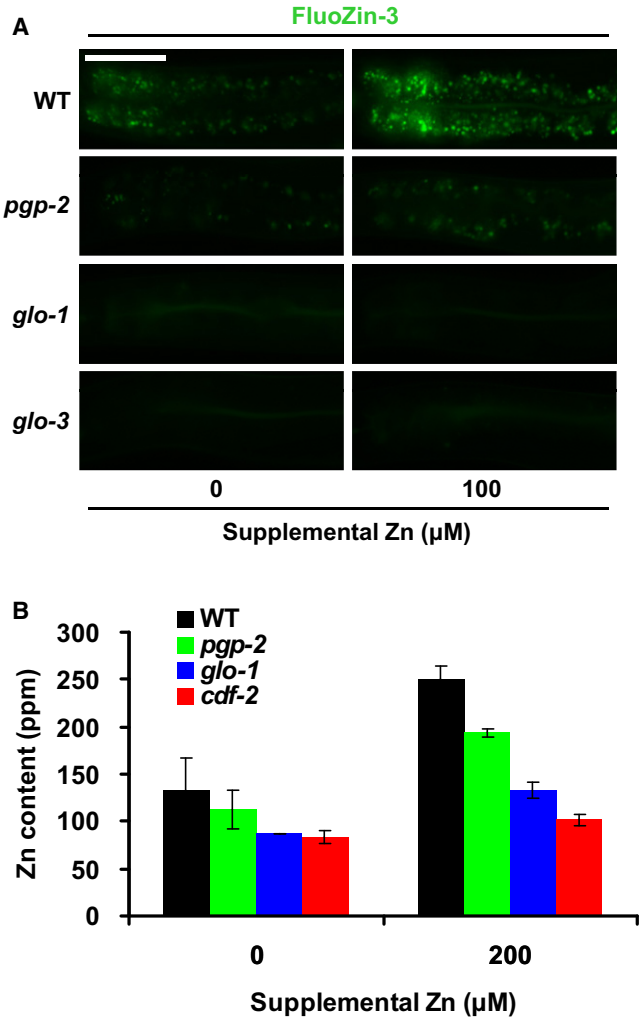

Figure 2. Gut Granules Are the Major Site of Zinc Storage

(A) Fluorescence images of live wild-type, *pgp-2*(*kx48*), *glo-1*(*zu391*), and *glo-3*(*zu446*) animals cultured with FluoZin-3 and the indicated levels of supplemental zinc. Images show the intestine with pharynx to the left and tail to the right. Scale bar: 50 μm.

(B) Total zinc content of wild-type, *pgp-2*(*kx48*), *glo-1*(*zu391*), and *cdf-2*(*tm788*) animals. Populations of animals consisting of a mixture of developmental stages were cultured on NAMM dishes with the indicated levels of supplemental zinc. Total zinc content was determined by ICP-MS and calculated in parts per million (ppm). Bars indicate mean values ± SEM of two independent experiments (see also Figure S3).

and 4.3-fold higher signal than control animals when cultured with 0 μM, 100 μM, and 200 μM supplemental zinc, respectively (Figure S2). These results indicate that the signal is primarily due to FluoZin-3 binding zinc with a minor contribution from autofluorescence.

Gut Granules Are the Major Site of Zinc Storage

To characterize the function of gut granules in zinc storage, we analyzed Glo mutant animals that have reduced numbers of gut granules due to defects in lysosome biogenesis. We analyzed three genes, *pgp-2*, *glo-1*, and *glo-3*, because well-characterized loss-of-function mutations in these genes cause Glo phenotypes of different severities; wild-type animals contain hundreds of gut granules, whereas *pgp-2(kx49)* animals contain 10–100 gut granules, and *glo-1(zu391)* and *glo-3(zu446)* animals contain fewer than 10 gut granules (Hermann et al., 2005; Rabbitts et al., 2008; Schroeder et al., 2007). *pgp-2* encodes an ABC transporter that localizes to the membrane of gut granules, *glo-1* encodes a predicted Rab GTPase that localizes to gut granules, and *glo-3* has not been molecularly identified. All three mutant strains displayed reduced FluoZin-3 fluorescence compared to wild-type (Figure 2A). Consistent with the severity of the Glo phenotype, *pgp-2* mutant animals displayed an intermediate number of FluoZin-3-positive granules, and *glo-1* and *glo-3* mutant animals displayed very few positive granules. These results indicate that gut granules are the site of labile zinc detected by FluoZin-3.

To quantify zinc storage defects in Glo animals, we measured total zinc content using the independent method of ICP-MS. *pgp-2* mutant animals displayed a moderate reduction of total zinc content, and *glo-1* mutant animals displayed a severe reduction of total zinc content compared to wild-type animals (Figure 2B). The total zinc content of the Glo animals was well correlated with the severity of the Glo phenotype. *glo-1* mutant animals cultured in high dietary zinc contained approximately 50% of the total zinc content of wild-type animals. These results indicate that gut granules are the major site of zinc storage in *C. elegans* that contains about half of the total zinc in the body. By contrast, Glo animals did not display a consistent change in total levels of magnesium, iron, manganese, or copper compared to wild-type animals (Figure S3). These results indicate that gut granules are specifically involved in zinc storage.

CDF-2 Promotes Zinc Storage in Gut Granules

The cation diffusion facilitator protein CDF-2 is expressed specifically in intestinal cells and localized to autofluorescent vesicles (Davis et al., 2009). To elucidate the relationship between CDF-2 and zinc storage, we cultured transgenic animals expressing CDF-2::mCherry with FluoZin-3. In animals cultured with no supplemental zinc, FluoZin-3 and CDF-2::mCherry fluorescence overlapped almost completely (Figure S4, left), indicating that CDF-2 is localized to the gut granules that concentrate zinc. *cdf-2* mRNA levels are increased by high dietary zinc (Davis et al., 2009). To analyze the regulation of CDF-2 protein expression by dietary zinc, we used transgenic animals expressing CDF-2::GFP. The level of CDF-2::GFP was induced in a concentration-dependent manner by approximately 3-fold and 4-fold at 100 μM and 200 μM supplemental zinc, respectively, compared to 0 μM supplemental zinc (Figures 3A and 3B). These results suggest that high levels of CDF-2 play an important role in the response to high dietary zinc.

To determine the function of CDF-2 in zinc storage in gut granules, we analyzed animals with the *cdf-2(tm788)* deletion mutation that causes a strong loss-of-function. *cdf-2(tm788)* mutant animals displayed significantly lower FluoZin-3 fluorescence at both 0 μM and 100 μM supplemental zinc compared to wild-type animals (Figures 3C and 3D). ICP-MS analysis revealed that *cdf-2(tm788)* mutant animals had a large reduction of total zinc content, similar to *glo-1* mutant animals (Figure 2B), consistent with our previous studies (Davis et al., 2009). These results indicate that CDF-2 is necessary to concentrate zinc

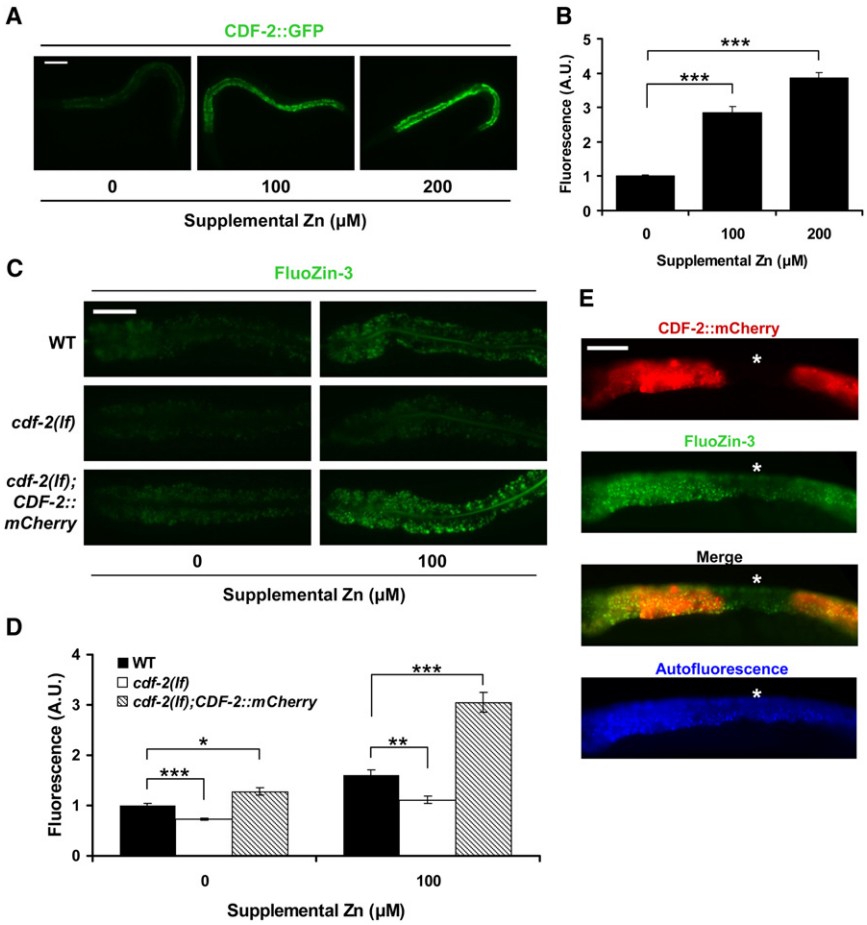

Figure 3. CDF-2 Functions Cell-Autonomously to Promote Zinc Storage in Gut Granules

(A) Fluorescence microscope images of live transgenic animals containing an integrated array, *amIs4*, expressing CDF-2::GFP, and the *cdf-2*(*tm788*) mutation. L4 stage hermaphrodites were cultured with the indicated levels of supplemental zinc. Each panel displays one representative animal oriented with pharynx to the left and tail to the right. Scale bar: 100 μm.

(B) Quantification of fluorescence images like those shown in (A). The fluorescence intensity (shown in arbitrary units, A.U.) was normalized by setting the value at 0 μM supplemental zinc equal to 1.0. Bars indicate mean values ± SEM (n = 15) (***p < 0.0001).

(C) Fluorescence microscope images of wild-type, *cdf-2*(*tm788*), and transgenic *cdf-2*(*tm788*) animals containing a multicopy extrachromosomal array; *amEx132*, expressing CDF-2::mCherry. Images show the intestine (pharynx to the left, tail to the right) of live animals cultured with FluoZin-3 and the indicated levels of supplemental zinc. Scale bar: 50 μm.

(D) Quantification of fluorescence images like those shown in (C). The fluorescence intensity (shown in arbitrary units, A.U.) was normalized by setting the value of wild-type animals at 0 μM supplemental Zn equal to 1.0. Bars indicate mean values ± SEM (n = 15) (*p < 0.01; **p < 0.001; ***p < 0.0001).

(E) Images of a live *cdf-2*(*tm788*);*amEx132* animal that displayed mosaic expression of the CDF-2::mCherry. The animal was cultured with FluoZin-3 and no supplemental zinc, and the intestine was imaged by fluorescence microscopy (pharynx to the left, tail to the right). The intestinal cell lacking CDF-2::mCherry expression is marked with a star (*). Scale bar: 50 μm (see also Figure S4).

into gut granules. *cdf-2(tm788)* mutant animals displayed slightly increased FluoZin-3 fluorescence at 100 μM compared to 0 μM supplemental zinc, suggesting that a CDF-2 independent mechanism might also promote zinc accumulation in gut granules. One possible mechanism is an alternative zinc transporter that might be induced in *cdf-2* mutant animals. *ttm-1* encodes a predicted CDF protein that is highly related to CDF-2 (H.C.R. and K.K., unpublished data). An analysis of *ttm-1* transcripts using qRT-PCR showed a small increase in *ttm-1* transcript levels in *cdf-2* mutant animals compared to wild-type animals (data not shown). Transgenic animals that contain multicopy, extrachromosomal arrays expressing CDF-2::mCherry displayed higher FluoZin-3 fluorescence compared to wild-type animals (Figures 3C and 3D). Thus, overexpression of CDF-2 was sufficient to concentrate zinc in gut granules.

Transgenic animals containing extrachromosomal arrays display mosaic expression of transgenes spontaneously and at a low frequency. To determine whether CDF-2 functions cell-autonomously, we analyzed mosaic animals that lack transgene expression in specific intestinal cells. Because these animals contain the *cdf-2(tm788)* mutation, an intestinal cell that lacks transgene expression lacks all CDF-2 function. The intestinal cells lacking CDF-2::mCherry expression displayed lower FluoZin-3 fluorescence compared to the flanking cells expressing CDF-2::mCherry (Figure 3E). These results indicate that CDF-2 functions cell-autonomously in intestinal cells to promote zinc concentration in gut granules.

High Dietary Zinc Alters Gut Granule Morphology

To characterize how the intracellular localization of CDF-2 responds to high dietary zinc, we examined the colocalization of CDF-2 and LysoTracker. With no supplemental zinc, CDF-2::GFP colocalized completely with LysoTracker (Figure 4A, left), demonstrating directly that CDF-2 localizes to the membrane of gut granules. In the presence of 200 μM supplemental zinc, CDF-2::GFP expression remained restricted to gut granules, but gut granules displayed altered morphology. Many vesicles had a bilobed appearance, and the two lobes displayed distinct staining patterns; one lobe was positive for both CDF-2 and LysoTracker, whereas the other lobe was positive for CDF-2 and negative for LysoTracker (Figure 4A, right). A dose response analysis showed that bilobed granules were induced by 100 μM and 200 μM supplemental zinc in worms cultured on NAMM dishes. The phenotype was highly penetrant, since bilobed granules were observed in nearly every animal, but only a subset of gut granules display a bilobed morphology.

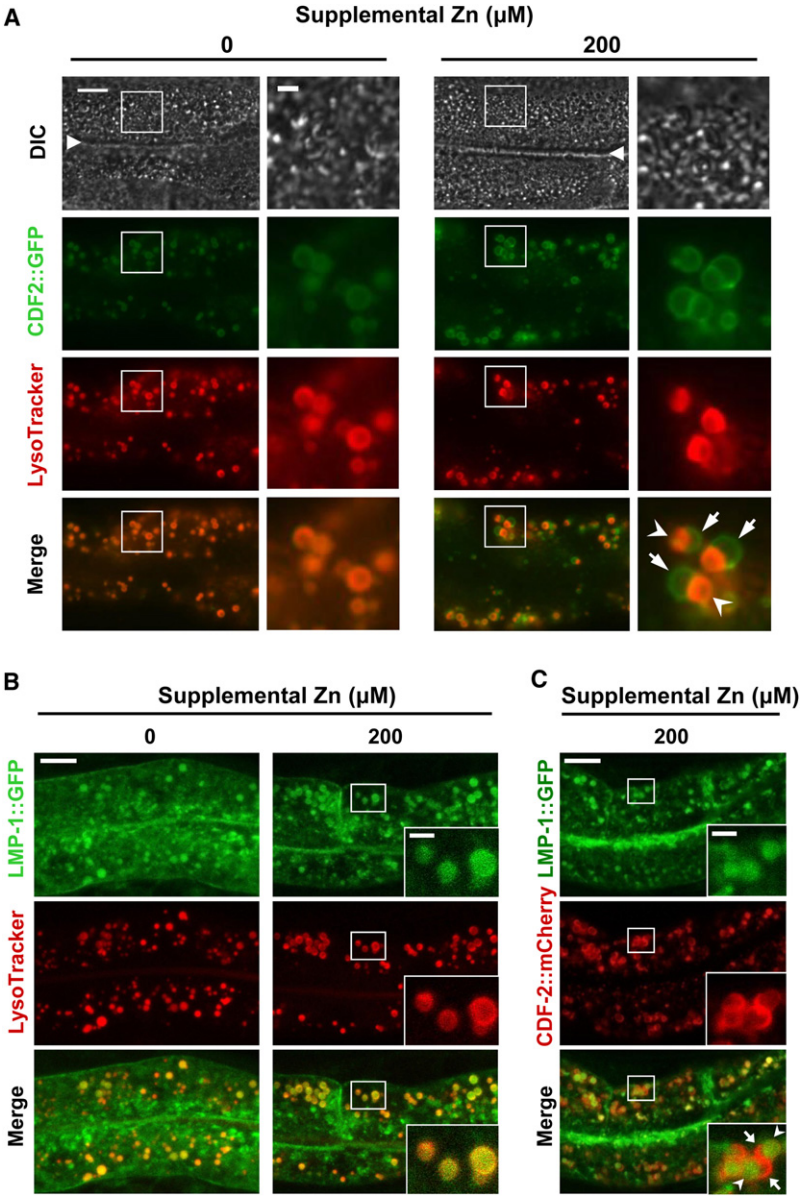

Figure 4. High Zinc Induces the Formation of Asymmetric Bilobed Gut Granules

(A) Fluorescence images of live transgenic animals expressing CDF-2::GFP cultured with LysoTracker and the indicated levels of supplemental zinc. The differential interference contrast (DIC) images show the intestinal lumen (triangle) and adjacent intestinal cells with pharynx to the left and tail to the right. Boxed regions are magnified in the right panels. With 200 μM supplemental zinc, many gut granules appear to be bilobed and asymmetric; one side is positive for CDF-2::GFP and LysoTracker (arrowhead), whereas the other side is positive for CDF-2::GFP and negative for LysoTracker (arrow). Scale bars: 10 μm and 2 μm (boxed regions) (see also Figure S5).

(B and C) Confocal microscope images of live transgenic animals expressing LMP-1::GFP cultured with LysoTracker (B) or expressing CDF-2::mCherry (C) cultured with the indicated levels of supplemental zinc. Images show intestinal cells with pharynx to the left and tail to the right. Insets are magnified images of the boxed regions. Scale bar: 10 μm and 2 μm (insets) (see also Figure S6).

Since LysoTracker labels acidic organelles, these results indicate that one lobe may lack the determinants that concentrate the LysoTracker or that the LysoTracker dye may be present but not fluorescent due to high pH. To examine a possible pH difference, we used LysoSensor Green DND-153, which is highly fluorescent in neutral compartments. Colocalization analysis with CDF-2::mCherry demonstrated that LysoSensor Green DND-153 was fluorescent only in one lobe of the bilobed gut granules (Figure S5), similar to LysoTracker staining. These results suggest that asymmetric staining of bilobed vesicles may reflect an asymmetric distribution of the molecules that bind these fluorescent probes.

To characterize additional differences between the two sides of bilobed gut granules, we first investigated the distribution of zinc using FluoZin-3. With 100 μM supplemental zinc, FluoZin-3 displayed asymmetric staining in bilobed gut granules; the LysoTracker-positive lobe displayed weak FluoZin-3 fluorescence, whereas the LysoTracker-negative lobe displayed strong FluoZin-3 fluorescence (Figure 1C, right). To examine the relationship between zinc levels and CDF-2 protein in bilobed gut granules, we examined the colocalization of FluoZin-3 and CDF-2::mCherry. While FluoZin-3 fluorescence was asymmetric and strong in only one lobe of bilobed granules, CDF-2::mCherry was localized to both lobes (Figure S4, right).

To define the molecular properties of bilobed gut granules, we examined the localization of several well-characterized endosomal or lysosomal marker proteins. The GTPase RAB-5 localizes to early endosomes (Chen et al., 2006; Hermann et al., 2005). RAB-5 did not colocalize with LysoTracker or CDF-2 (data not shown), suggesting that gut granules are distinct from early endosomes. Lysosome associated membrane proteins (LAMPs) are localized predominantly in lysosomes in vertebrates, and *C. elegans* LMP-1 localizes to late endosomal or lysosomal vesicles of intestinal cells (Chen et al., 2006; Kostich et al., 2000). A subset of LMP-1 colocalized with LysoTracker in gut granules (Figure 4B). In addition, a subset of LMP-1 localized to other membrane compartments that were LysoTracker negative, including the plasma membrane, indicating this marker is not specific for lysosomes. To determine whether LMP-1 was present on both lobes of bilobed gut granules, we exposed worms to high zinc and used CDF-2::mCherry to define bilobed morphology. LMP-1 was present only in one lobe of bilobed gut granules (Figure 4C). These results indicate that bilobed gut granules displayed asymmetric molecular properties; one lobe has late endosomal or lysosomal characteristics whereas the other lobe lacks at least one lysosomal protein.

C. elegans PGP-2 is an ABC transporter that localizes specifically to the gut granule membrane (Schroeder et al., 2007). With

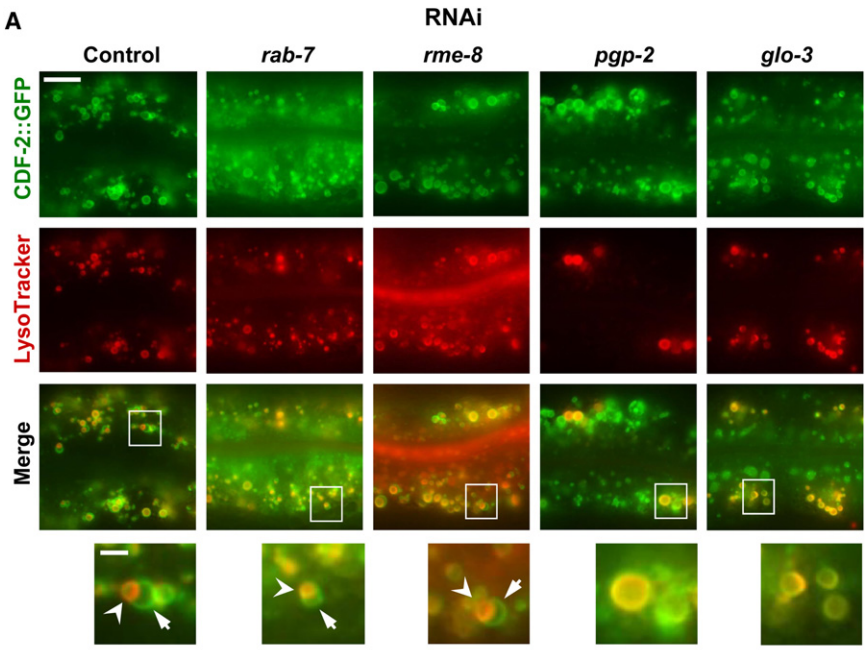

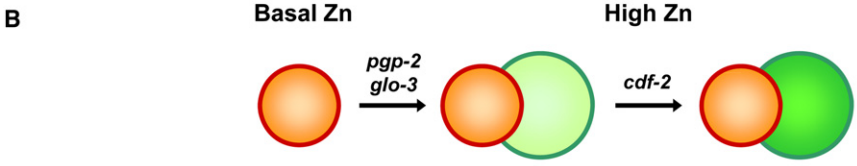

Autofluorescence	+		+	-
LysoTracker	+		+	-
LysoSensor DND-153	+		+	-
RAB-5	-		-	-
LMP-1	+		+	-
PGP-2	+		+	+
CDF-2	+		+	+
Labile Zinc (FluoZin-3)	Low		Low	High

Figure 5. *Glo* Genes Are Necessary for the Formation of Bilobed Gut Granules

(A) Fluorescence microscope images of live transgenic animals expressing CDF-2::GFP. L1 stage animals were fed RNAi bacteria to reduce expression of the indicated genes, and L4 stage animals were cultured with LysoTracker and 200 μM supplemental zinc for ~16 hr and visualized. Images show intestinal cells with pharynx to the left and tail to the right. Boxed regions are magnified in the bottom panels. Bilobed gut granules are indicated by arrows and arrowheads. Scale bar: 10 μm and 2 μm (bottom) (see also Figure S7).

(B) A genetic pathway for the formation of bilobed gut granules and a summary of molecular properties of gut granules in basal zinc (left) and bilobed gut granules in high zinc (right). Plus (+) and minus (−) signs indicate the presence and absence of proteins/staining, respectively. Low and high indicate relative levels of FluoZin-3 staining.

no supplemental zinc, CDF-2::mCherry, PGP-2::GFP, and autofluorescence completely colocalized in gut granules (Figure S6B, left). With 100 μM supplemental zinc, CDF-2 and PGP-2 fully colocalized on both sides of bilobed gut granules, while autofluorescence displayed an asymmetric pattern and was only prominent on one lobe, similar to the LysoTracker staining pattern (Figure S6B, right). These results indicate that bilobed gut granules contain proteins that are distributed on both lobes, such as PGP-2 and CDF-2, and at least one protein that is asymmetrically localized to the LysoTracker positive lobe, LMP-1 (Figure 5B).

Glo Genes Are Necessary for the Formation of Bilobed Gut Granules

To elucidate the role of vesicular trafficking pathways in bilobed gut granule formation, we reduced the activity of key genes using the method of feeding RNAi. Animals were exposed to RNAi starting at the first larval (L1) stage to allow normal embryonic development. RAB-7 and RME-8 are necessary for lysosome biogenesis and endocytosis in multiple cell types (Bucci et al., 2000; Zhang et al., 2001), although a function in adult intestinal cells has not been reported. When *rab-7* or *rme-8* activities were reduced by RNAi, bilobed morphology was still detected (Figure 5A), indicating that these genes may not be required for the formation of bilobed gut granules or that residual gene activity was sufficient to mediate formation of bilobed granules. When *pgp-2* or *glo-3* activities were reduced by RNAi, bilobed morphology was not observed (Figure 5A). We did observe vesicles that contained CDF-2::GFP and were LysoTracker negative, which we have not observed in wild-type animals. These results suggest that *glo* genes that function in gut granule biogenesis are also required for the formation of bilobed morphology in response to high zinc.

To determine the role of zinc transport in the formation of bilobed gut granules, we analyzed *cdf-2*. *cdf-2* mutant animals displayed bilobed gut granules that contained PGP-2::GFP on both lobes and LysoTracker asymmetrically on one lobe (Figure S7A), similar to wild-type. In contrast to wild-type, bilobed gut granules were not stained asymmetrically with FluoZin-3 in *cdf-2* mutant animals (Figure S7B). These results indicate that CDF-2 activity is not necessary for the formation of bilobed gut granules but is necessary for the asymmetric accumulation of zinc. These results define a genetic pathway for the formation of bilobed organelles (Figure 5B).

Gut Granules Are Necessary for Zinc Detoxification

To determine if zinc storage in gut granules is a protective mechanism that promotes detoxification, we analyzed the ability of

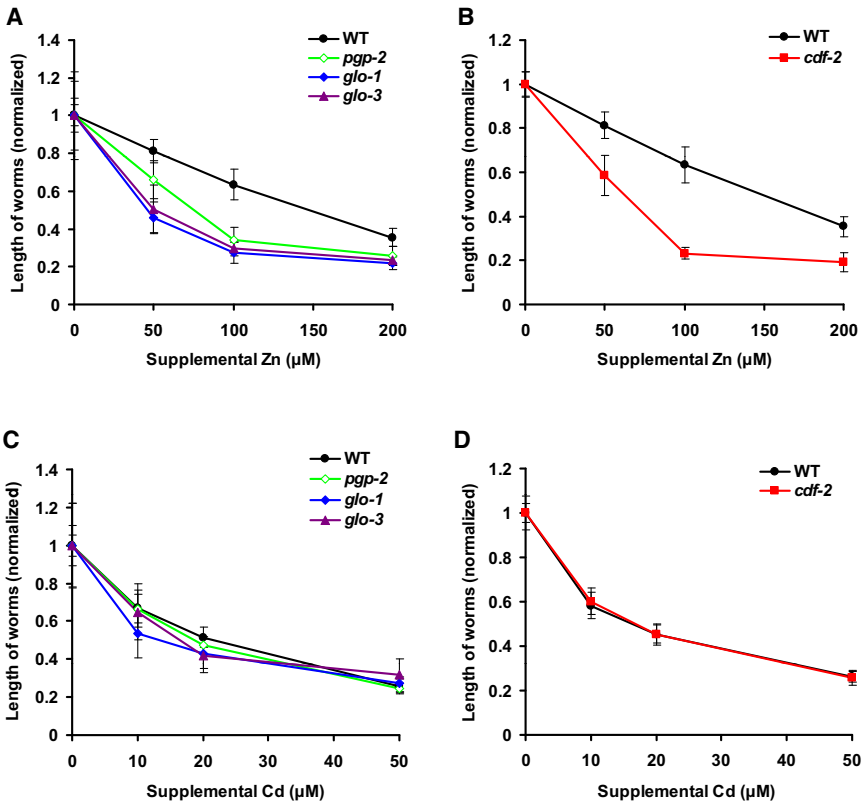

Figure 6. Zinc Storage in Gut Granules Promotes Detoxification

(A–D) Wild-type, *pgp-2(kx48)*, *glo-1(zu391)*, *glo-3(zu446)*, and *cdf-2(tm788)* hermaphrodites were synchronized at the L1 stage and cultured on NAMM dishes for 3 days with the indicated levels of supplemental zinc in (A and B) or supplemental cadmium (C and D). The length of individual animals was measured using microscopy and ImageJ software. To compare strains that have different growth rates under optimal conditions, we normalized the length of worms by setting the value at 0 μM supplemental metal equal to 1.0 for each strain. Each point indicates mean values ± SD (n = 10 for Zn, and n = 20 for Cd).

animals to tolerate high levels of dietary zinc. Dose-dependent zinc toxicity was previously determined using fully defined liquid CeMM medium (Davis et al., 2009). Here, we show that wild-type animals cultured on NAMM dishes displayed a dose-dependent decrease in growth rate in response to supplemental zinc, indicating that high dietary zinc inhibits growth in a different culture medium (Figure 6A). The concentration of zinc in these two experiments cannot be compared directly due to differences in culture conditions, particularly the undefined contribution of bacteria to dietary zinc for worms cultured on NAMM dishes. *pgp-2, glo-1*, and *glo-3* mutant animals displayed significantly lower growth rates than wild-type animals at all concentrations of supplemental zinc (Figure 6A). The severity of the zinc sensitivity phenotype correlated with the severity of Glo phenotype; *pgp-2* mutant animals were moderately zinc sensitive, whereas *glo-1* and *glo-3* mutant animals were strongly zinc sensitive. These results indicate that gut granules play an important protective role in response to zinc toxicity. To test the hypothesis that zinc storage in gut granules is important for zinc resistance rather than another function of gut granules, we analyzed *cdf-2. cdf-2(tm788)* mutant animals appeared to have a normal number and morphology of gut granules based on LysoTracker and PGP-2::GFP staining, but these granules were defective in zinc storage (Figure S7). Similar to Glo animals, *cdf-2* mutant animals were hypersensitive to dietary zinc compared to wild-type animals (Figure 6B). These findings indicate that CDF-2 mediated zinc transport into gut granules is a critical mechanism for zinc detoxification.

To investigate whether gut granules play a more general role in metal detoxification, we examined the sensitivity of Glo animals to the toxic effects of additional metals. Glo animals were similar to wild-type animals in sensitivity to dietary cadmium (Figure 6C) and copper (data not shown), indicating that gut granules are not necessary to detoxify these metals. The growth of *cdf-2(tm788)* mutant animals was also similar to wild-type animals in the presence of supplemental cadmium (Figure 6D) and copper (data not shown). These results indicate that CDF-2 function is specific to zinc and support the conclusion that gut granules are not a general site of metal storage and may be specific for zinc storage.

Gut Granules Provide a Source of Zinc during Deficiency

One possible function of storing zinc in gut granules is to provide a source of zinc that can be mobilized in response to zinc deficiency. To test this model, we monitored the levels of zinc in gut granules using FluoZin-3 during a shift from high zinc to low zinc conditions. Wild-type animals cultured with 200 μM supplemental zinc were transferred to NAMM dishes containing 200 μM supplemental zinc, 0 μM supplemental zinc, or 100 μM TPEN and analyzed for FluoZin-3 fluorescence after 24 hr and 48 hr. Animals continuously cultured with 200 μM supplemental zinc displayed a progressive increase of FluoZin-3 fluorescence (Figures 7A and 7B). Animals shifted to 0 μM supplemental zinc displayed FluoZin-3 fluorescence that increased by ~1.7-fold after 24 hr but then slightly decreased after 48 hr. Animals shifted to 100 μM TPEN displayed FluoZin-3 fluorescence that increased by ~1.4-fold after 24 hr but then substantially decreased after 48 hr to a level below the initial value. These results suggest that zinc stored in gut granules is released during zinc deficiency.

To investigate the physiologic significance of zinc mobilization, we analyzed the growth of animals that had either low or high zinc storage and then were exposed to zinc-deficient conditions. Wild-type animals were precultured with either 0 μM or 50 μM supplemental zinc and then cultured in the presence of TPEN. Animals precultured with 50 μM supplemental zinc displayed a significantly increased growth rate in 100 μM TPEN compared to animals precultured with 0 μM

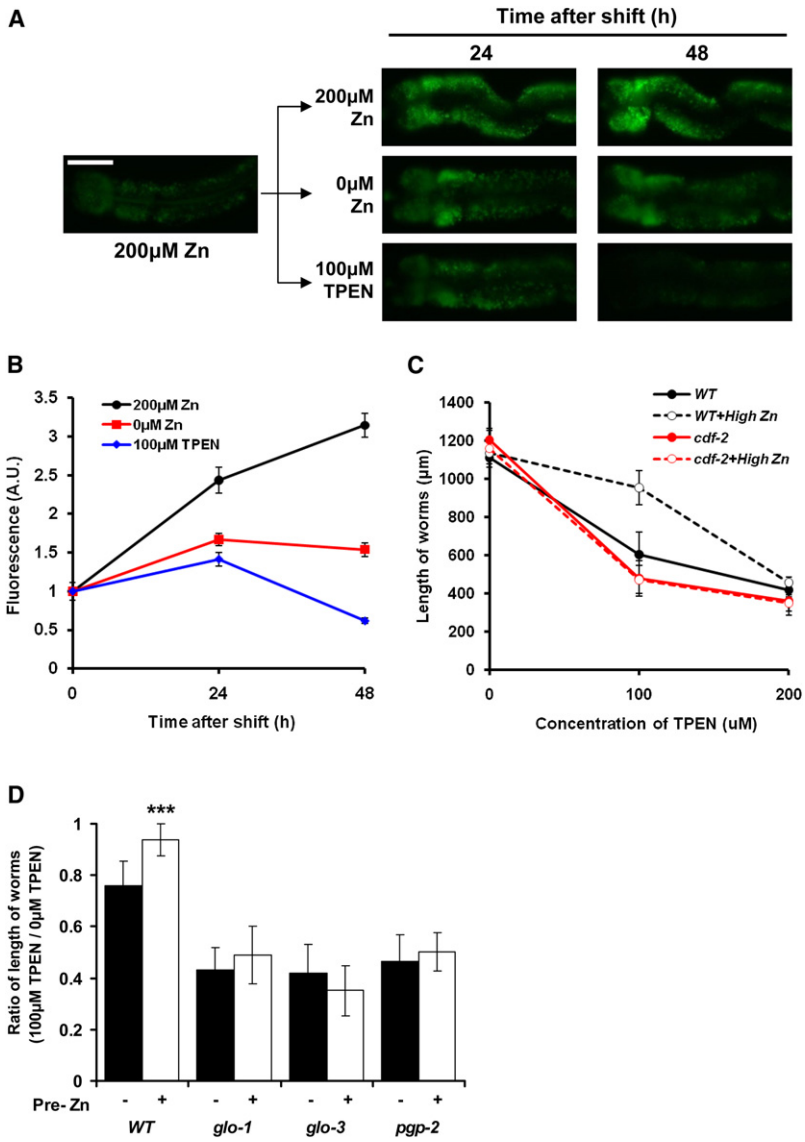

Figure 7. Zinc in Gut Granules Can Be Mobilized in Response to Zinc Deficiency

(A) Wild-type L4 stage hermaphrodites were cultured on NAMM dishes containing 200 μM supplemental zinc to promote zinc storage. Animals were then transferred to NAMM dishes containing the indicated levels of supplemental zinc or TPEN, and FluoZin-3 fluorescence was analyzed by fluorescence microscopy after 24 hr and 48 hr. Images show intestinal cells (pharynx to the left and tail to the right). Scale bar: 50 μm.

(B) Quantification of fluorescence images like those shown in (A). The fluorescence intensity (shown in arbitrary units, A.U.) was normalized by setting the value at 200 μM supplemental Zn (time 0) equal to 1.0. Each point indicates mean values ± SEM (n = 10).

(C) Wild-type and *cdf-2*(*tm788*) L1 stage hermaphrodites were precultured for 12 hr on NAMM dishes containing 0 or 50 μM supplemental zinc (High Zn), cultured for 3 days on NGM dishes with the indicated levels of TPEN, and analyzed individually for length. Each point indicates mean value ± SD (n = 20).

(D) Wild-type, *glo-1*(*zu391*), *glo-3*(*zu446*) and *pgp-2*(*kx48*) animals were analyzed as described in (C). The results with 100 μM TPEN are presented, because this concentration was the most informative with wild-type animals. The length of individual worms at 100 μM TPEN was divided by the average length at 0 μM TPEN. Bars indicate mean values ± SD (n = 20). This ratio compares the growth of worms in deficient and normal zinc conditions—lower values indicate more severely reduced growth in response to zinc deficiency. Animals were precultured with 0 (black) or 50 μM (white) supplemental zinc. For each strain, the white bar was compared to the black bar (***p < 0.0001). All the mutant strain black and white bar values were significantly different than the wild-type black and white bar values, respectively.

supplemental zinc (Figure 7C), indicating that stored zinc can be mobilized during dietary deficiency. *cdf-2* mutant animals precultured with 50 μM supplemental zinc did not display a significant increase in growth rate (Figures 7C). These results indicate that CDF-2 is necessary for zinc storage, which promotes the resistance to zinc deficiency. To determine if zinc is mobilized from gut granules during deficiency, we examined Glo animals. *glo-1, glo-3*, and *pgp-2* mutant animals precultured with 0 μM supplemental zinc displayed slower growth rates in the presence of TPEN compared to wild-type animals (Figure 7D). In addition, the growth rate of the Glo animals was not significantly affected by preculture with 50 μM supplemental zinc, whereas wild-type animals displayed a significant increase (Figure 7D). These results indicate that gut granules, which are the major site of zinc storage during dietary excess, are the source of zinc mobilized during zinc deficiency.

DISCUSSION

Lysosome-Related Organelles Are a Site of Zinc Storage and Mobilization in an Animal

Zinc is essential, but zinc availability can fluctuate. Thus, mechanisms to store and mobilize zinc are important. We used *C. elegans* to characterize the site of zinc storage in an animal by developing methods to visualize labile zinc using a zinc-specific fluorescent dye, FluoZin-3. Labile zinc was detected primarily in lysosome-related organelles in intestinal cells called gut granules. The biogenesis of gut granules has been studied using Glo mutant animals that have reduced numbers of gut granules (Hermann et al., 2005; Rabbitts et al., 2008; Schroeder et al., 2007). Glo mutant animals were used to demonstrate that reducing the number of gut granules caused a corresponding reduction of labile and total zinc. By contrast, Glo mutant animals had wild-type levels of other metals such as copper. These results indicate that gut granules function specifically in zinc storage and provide direct evidence for the presence of a zinc-specific storage site in an animal.

The cation diffusion facilitator protein CDF-2 plays a critical role in zinc storage in these organelles. Colocalization experiments with gut granule markers demonstrated that CDF-2 is

localized specifically to the membrane of gut granules. The level of CDF-2 protein was increased by high dietary zinc, indicating CDF-2 has an important function in responding to high levels of zinc. This function was demonstrated using genetic analysis, since reducing the activity of *cdf-2* with a loss-of-function mutation and increasing the activity of *cdf-2* by overexpression showed that *cdf-2* is both necessary and sufficient for zinc storage in gut granules. Consistent with the model that CDF-2 directly transports zinc into gut granules, CDF-2 functioned cell-autonomously in intestinal cells to promote zinc accumulation. The protein sequence of *C. elegans* CDF-2 is similar to mammalian ZnT-2, which was discovered by Palmiter et al. (1996) and shown to promote cellular resistance to zinc by facilitating vesicular sequestration in cultured cells. Similar to CDF-2, ZnT-2 is localized to intracellular organelles and regulated by dietary zinc (Falcón-Pérez and Dell'Angelica, 2007; Guo et al., 2010; Liuzzi et al., 2001). Mutations in human ZnT-2 are associated with low milk zinc concentrations, indicating one function of ZnT-2 in humans is secretion of zinc into breast milk (Chowanadisai et al., 2006). These similarities suggest that *C. elegans* CDF-2 and mammalian ZnT-2 have important and conserved functions in cellular and organismal zinc metabolism.

We characterized two functions of zinc storage in gut granules. One function is detoxification. Glo mutant animals that had reduced numbers of gut granules were hypersensitive to zinc toxicity, and the hypersensitivity correlated with the severity of the Glo phenotype, demonstrating the importance of gut granules in zinc tolerance. *cdf-2* loss-of-function mutant animals had normal numbers of gut granules, but these organelles were deficient in zinc accumulation, and *cdf-2* mutant animals were also hypersensitive to dietary zinc. Thus, CDF-2-mediated transport of zinc into gut granules is a key mechanism to detoxify excess dietary zinc. In the unicellular yeast *Saccharomyces cerevisiae*, the vacuole plays an important role in zinc tolerance, and zinc transport into the vacuole is mediated by the CDF proteins Cot1 and Zrc1 (Eide, 2006). Acidocalcisomes are specialized organelles that accumulate zinc and other metals and have been observed in a wide range of organisms (Docampo et al., 2005). In vertebrates, several cell types have been shown to accumulate zinc in specific organelles. For example, glutamatergic neurons, pancreatic β-cells and acinar cells, and intestinal paneth cells contain secretary vesicles with high concentrations of labile zinc (Kelly et al., 2004; Lichten and Cousins, 2009). Dietary zinc levels influence the number of paneth cells and the morphology of the zinc-containing organelles, suggesting there may be parallels with the gut granules of *C. elegans* intestinal cells (Kelly et al., 2004). In several types of mammalian cells, labile zinc accumulates in intracellular organelles that have lysosomal properties and have been called zincosomes (Haase and Beyersmann, 1999; Palmiter et al., 1996). ZnT-2 mediates zinc transport into zincosomes and promotes zinc tolerance (Falcón-Pérez and Dell'Angelica, 2007). Because yeast vacuoles, *C. elegans* gut granules, and mammalian zincosomes all have lysosomal properties, lysosome-related organelles may have an evolutionarily conserved function in cellular zinc storage. High levels of dietary zinc induce changes in gene expression, such as induction of metallothionein genes, and these alterations in gene expression may play a role in detoxification (Andrews, 2001). An important direction for future research will be to determine how zinc sequestration in lysosome-related organelles relates to other mechanisms of zinc tolerance such as expression of zinc-binding proteins.

The second function of zinc storage in gut granules is to provide a source of zinc that can be mobilized during dietary deficiency. Animals shifted from high to low zinc conditions displayed decreased zinc levels in gut granules after 48 hr, suggesting that stored zinc is released in response to deficiency. Importantly, our data indicate that stored zinc is utilized for the physiologic process of growth, since wild-type animals with normal zinc storage grew more robustly than Glo and *cdf-2* mutant animals with defective zinc storage. These results demonstrate the existence of a specific site of zinc storage in an animal that provides a physiologically important source of zinc during dietary deficiency. Elegant studies reported by Eide and colleagues show that zinc stored in the yeast vacuole is mobilized by the ZIP protein Zrt3, and stored zinc can supply the needs of as many as eight generations of progeny cells under zinc starvation conditions (MacDiarmid et al., 2000; Simm et al., 2007). In mammalian T cells, ZIP8 localizes to lysosomes and mediates release of zinc that plays a regulatory role in T cell activation (Aydemir et al., 2009; Begum et al., 2002). Zinc storage and mobilization at the organismal level has been investigated in vertebrates. Chickens fed a high zinc diet display accumulation of zinc in several tissues including the liver, bone, and small intestine (Emmert and Baker, 1995). When these animals are shifted to a zinc-deficient diet, the level of accumulated zinc decreases, and the onset of zinc deficiency symptoms is delayed compared to control chickens fed a low zinc diet, suggesting that accumulated zinc may be mobilized. In humans, symptoms of zinc deficiency develop rapidly in response to dietary zinc deficiency, indicating there are only small pools of zinc available for mobilization (King, 2011). Our studies indicate that the capacity for zinc storage and mobilization of *C. elegans* is intermediate between the large capacity of yeast and the small capacity of mammals. The limited capacity of animals compared to yeast may reflect the strategy of storing zinc in specialized cell types, such as intestinal cells in *C. elegans*, compared to storage in the vacuole of every yeast cell.

Lysosome-Related organelles Adopt a Bilobed Morphology in Response to High Zinc

Gut granules displayed striking morphological changes in response to high dietary zinc. In standard culture conditions, gut granules were typically round in shape, autofluorescent, positive for LysoTracker and FluoZin-3 staining, and positive for membrane localization of CDF-2, LMP-1, and PGP-2. In high dietary zinc, gut granules were frequently bilobed in shape, and the two lobes displayed an asymmetric distribution of molecules. One lobe displayed molecular properties that were similar to gut granules in standard culture conditions, whereas the other lobe displayed strong FluoZin-3 staining, was positive for the gut granule-specific proteins PGP-2 and CDF-2, and was negative for the lysosomal markers Lysotracker and LMP-1. The high level of zinc in one lobe raises the possibility that CDF-2 is more abundant or active in the high zinc lobe. Using epifluorescence microscopy, CDF-2 levels appeared to be similar on both lobes. However, this analysis is complicated by autofluorescence from the LysoTracker positive lobe. Using confocal microscopy that

minimizes signal due to autofluorescence, CDF-2 levels appeared to be higher on the lobe with high zinc, suggesting that there may be a positive correlation between CDF-2 levels and zinc accumulation. While these studies are suggestive, strong conclusions about the relative levels of CDF-2 on the two lobes will require a more quantitative analysis than described here. We speculate that the bilobed structure may facilitate zinc storage by generating a compartment that is specialized to accommodate a large amount of zinc. Alternatively, it may facilitate zinc excretion through budding of a secretory vesicle containing excess zinc. Secretory granules of mammalian paneth cells also display nonhomogenous staining of the contents, but the arrangement is distinct from the bilobed granules. Based on EM analysis, paneth cell granules have a central core and a distinct surround, called a biphasic structure, which differ in carbohydrate composition (Leis et al., 1997).

We used genetic analysis to elucidate a pathway for the formation of bilobed gut granules (Figure 5B). Reducing the activity of *pgp-2* and *glo-3* by the method of RNAi inhibited the formation of bilobed morphology. Because *glo* genes were inactivated after gut granule biogenesis during embryonic development, the absence of bilobed morphology is not likely to be caused by defects in gut granule biogenesis. Rather, *glo* genes are likely to act in both gut granule biogenesis and the transition to bilobed morphology in response to high levels of zinc. Interestingly, animals exposed to RNAi of *glo* genes displayed vesicles that contained CDF-2::GFP and were LysoTracker negative. These vesicles were spatially separate from gut granules that contained CDF-2::GFP and were LysoTracker positive, suggesting that *glo* genes may be involved in a vesicle fusion event that generates bilobed morphology. *cdf-2* mutant animals displayed organelles with bilobed morphology, based on membrane staining with PGP-2, but these organelles did not display FluoZin-3 fluorescence. Thus, CDF-2 is not necessary for the formation of bilobed morphology but is necessary to accumulate zinc in bilobed organelles. Therefore, the formation of bilobed morphology is separable from zinc transport and accumulation. Lysosome biogenesis and function can be regulated by signaling pathways in response to cellular conditions (Karageorgos et al., 1997), and the transcription factor EB was recently demonstrated to play a critical role in this process (Sardiello et al., 2009). These results indicate lysosomes are not static organelles, but rather respond dynamically to cellular conditions. Our results showed that environmental zinc induced transcription of *cdf-2*, a resident protein of lysosome-related organelles, and caused lysosome-related organelles to adopt a bilobed morphology. These findings are consistent with the model that the transcriptional response to environmental zinc causes dynamic changes in lysosome-related organelle structure and function. These studies establish a genetically tractable model system to dissect the contribution of transcriptional programs to the biogenesis of specialized lysosome-related organelles that play a critical role in coping with the environmental challenge of high zinc.

EXPERIMENTAL PROCEDURES

General Methods and Strains

C. elegans strains were cultured at 20°C on nematode growth medium (NGM) seeded with *E. coli* OP50 unless otherwise noted (Brenner, 1974). The wild-type *C. elegans* and parent of all mutant strains was Bristol N2. The following mutations and transgenes were used: *pgp-2*(*kx48*) *I* (Schroeder et al., 2007), *unc-119*(*ed3*) *III* (Praitis et al., 2001), *cdf-2*(*tm788*) *X* (Davis et al., 2009), *glo-1*(*zu391*) *X* (Hermann et al., 2005), *glo-3*(*zu446*) *X* (Rabbitts et al., 2008), *amIs4*(*cdf-2::GFP::unc-119*(+)) (Davis et al., 2009), *pwIs50* (*lmp-1:GFP*) (Treusch et al., 2004), *pwIs72* (*Pvha-6::GFP::rab-5*) (Hermann et al., 2005), and *kxEx98*(*pgp-2::GFP;rol-6^{D}*) (Schroeder et al., 2007). *amEx132*(*cdf-2::mCherry;rol-6^{D}*) and *amEx142*(*cdf-2::mCherry::unc-119*(+)) are described here. Double mutant animals were generated by standard methods, and genotypes were confirmed by PCR or DNA sequencing.

Metal Sensitivity Assays

Gravid adult hermaphrodites were treated with NaOH and bleach, and eggs were incubated in M9 solution overnight to allow hatching and synchronized arrest at the L1 stage. L1 animals were transferred to NAMM dishes (Bruinsma et al., 2008) supplemented with zinc sulfate ($ZnSO_4$), cadmium chloride ($CdCl_2$), or copper sulfate ($CuSO_4$) and seeded with concentrated OP50. After 3 days, animals were washed twice in M9 containing 0.01% Tween-20, paralyzed with 10 mM sodium azide (NaN_3) in M9, and mounted on a 2% agarose pad on a microscope slide. Images were captured with a Zeiss Axioplan 2 microscope equipped with a Zeiss AxioCam MRm digital camera. Length of individual animals was measured as an indicator of growth using ImageJ software (NIH) by drawing a line from the nose to the tail tip.

Quantitative Analysis of CDF-2::GFP Expression by Fluorescence Microscopy

cdf-2(tm788);amIs4 animals were synchronized at L1 stage and cultured on NGM dishes. L4 stage hermaphrodites were then cultured for 24 hr on NAMM dishes supplemented with $ZnSO_4$ and seeded with concentrated OP50. Animals were paralyzed with 0.1% tricaine and 0.01% tetramisole in M9, mounted on 2% agarose pads on microscope slides, and imaged with a Zeiss Axioplan 2 microscope equipped with a Zeiss AxioCam MRm digital camera using identical settings and exposure times. GFP fluorescence intensity was quantified using ImageJ software (NIH). Briefly, the Spot Enhancing Filter 2D plugin was used to amplify signals from gut granules, and then threshold settings were used to specifically select the fluorescent regions of gut granules. The selected regions were overlaid on the original images and analyzed for mean fluorescence intensity of the area.

Staining with FluoZin-3, LysoTracker, and LysoSensor

FluoZin-3 acetoxymethyl (AM) ester (Molecular Probes F24195) was reconstituted in dimethylsulfoxide (DMSO) to generate a 1 mM stock solution, diluted in M9 and dispensed on NAMM dishes to yield a final concentration of 3 μM. L4 stage hermaphrodites were cultured on these dishes for 12–24 hr in the dark, transferred to NGM dishes without FluoZin-3 for 30 min to reduce FluoZin-3 in the intestinal lumen, and analyzed by fluorescence microscopy as described above. The intestine on the anterior half of each animal was analyzed because this structure was typically observed in the same focal plane. Residual fluorescence from the intestinal lumen was manually removed and excluded from the analysis.

LysoTracker RED DND-99 (1 mM, Invitrogen L7528), or LysoSensor Green DND-153 (1 mM, Invitrogen L7534) were diluted in M9 and dispensed on NAMM dishes to yield a final concentration of 2 μM. L4 stage hermaphrodites were cultured on these dishes for 12–24 hr in the dark, transferred to NGM dishes without dye for 30 min, and imaged as described above. Confocal microscopy was performed using an Olympus FV500 confocal microscope system equipped with multiline argon (458/488/515 nm) and krypton (568 nm) lasers.

Zinc Shift Assays

To monitor zinc levels in gut granules, we cultured L4 stage animals for 12–16 hr on NAMM dishes containing FluoZin-3 and 200 μM $ZnSO_4$ and then analyzed them by fluorescence microscopy as described above. Next, animals were transferred to NAMM dishes with FluoZin-3 containing 0 or 200 μM ZnSO4 or 100 μM TPEN and analyzed by fluorescence microscopy after 24 hr and 48 hr. To analyze growth, we cultured synchronized L1 stage animals on NAMM dishes supplemented with 0 or 50 μM $ZnSO_4$ for 12 hr. We chose 50 μM supplemental zinc because it caused relatively mild toxicity

as measured by subsequent growth, whereas 100 and 200 μM supplemental zinc caused substantial toxicity (data not shown). Animals were washed three times, incubated in M9 containing 0.01% Tween-20 for 30 min to minimize residual bacteria, and washed one time in M9 containing 0.01% Tween-20. Animals were cultured for 3 days on NGM dishes supplemented with TPEN and seeded with concentrated OP50, and the length of each animal was determined.

Statistics

All data were analyzed by two-tailed unpaired Student's t test, and $p < 0.05$ was considered statistically significant.

SUPPLEMENTAL INFORMATION

Supplemental Information includes seven figures, Supplemental Experimental Procedures, and Supplemental References and can be found with this article online at doi:10.1016/j.cmet.2011.12.003.

ACKNOWLEDGMENTS

We thank Greg Hermann, Barth Grant, the Caenorhabditis Genetics Center, and the National Bioresource Project for providing strains; Andrew Fire, Michael Nonet, and Judith Austin for providing plasmids; and Daniel Schneider for technical assistance. We are grateful to Tim Schedl, Stuart Kornfeld, Jeanne Nerbonne, Jason Mills, and Peter Chivers for helpful advice about the manuscript. This research was supported by grants from the National Institutes of Health to K.K. (GM068598, CA84271, and AG026561). K.K. was a Senior Scholar of the Ellison Medical Foundation. H.C.R. was a scholar of the McDonnell International Scholars Academy.

Received: July 7, 2010
Revised: October 3, 2011
Accepted: December 2, 2011
Published online: January 3, 2012

REFERENCES

Andrews, G.K. (2001). Cellular zinc sensors: MTF-1 regulation of gene expression. Biometals *14*, 223–237.

Aydemir, T.B., Liuzzi, J.P., McClellan, S., and Cousins, R.J. (2009). Zinc transporter ZIP8 (SLC39A8) and zinc influence IFN-gamma expression in activated human T cells. J. Leukoc. Biol. *86*, 337–348.

Begum, N.A., Kobayashi, M., Moriwaki, Y., Matsumoto, M., Toyoshima, K., and Seya, T. (2002). Mycobacterium bovis BCG cell wall and lipopolysaccharide induce a novel gene, BIGM103, encoding a 7-TM protein: identification of a new protein family having Zn-transporter and Zn-metalloprotease signatures. Genomics *80*, 630–645.

Brenner, S. (1974). The genetics of *Caenorhabditis elegans*. Genetics *77*, 71–94.

Bruinsma, J.J., Jirakulaporn, T., Muslin, A.J., and Kornfeld, K. (2002). Zinc ions and cation diffusion facilitator proteins regulate Ras-mediated signaling. Dev. Cell *2*, 567–578.

Bruinsma, J.J., Schneider, D.L., Davis, D.E., and Kornfeld, K. (2008). Identification of mutations in *Caenorhabditis elegans* that cause resistance to high levels of dietary zinc and analysis using a genomewide map of single nucleotide polymorphisms scored by pyrosequencing. Genetics *179*, 811–828.

Bucci, C., Thomsen, P., Nicoziani, P., McCarthy, J., and van Deurs, B. (2000). Rab7: a key to lysosome biogenesis. Mol. Biol. Cell *11*, 467–480.

Chen, C.C., Schweinsberg, P.J., Vashist, S., Mareiniss, D.P., Lambie, E.J., and Grant, B.D. (2006). RAB-10 is required for endocytic recycling in the Caenorhabditis elegans intestine. Mol. Biol. Cell *17*, 1286–1297.

Chowanadisai, W., Lönnerdal, B., and Kelleher, S.L. (2006). Identification of a mutation in SLC30A2 (ZnT-2) in women with low milk zinc concentration that results in transient neonatal zinc deficiency. J. Biol. Chem. *281*, 39699–39707.

Clokey, G.V., and Jacobson, L.A. (1986). The autofluorescent "lipofuscin granules" in the intestinal cells of *Caenorhabditis elegans* are secondary lysosomes. Mech. Ageing Dev. *35*, 79–94.

Cragg, R.A., Phillips, S.R., Piper, J.M., Varma, J.S., Campbell, F.C., Mathers, J.C., and Ford, D. (2005). Homeostatic regulation of zinc transporters in the human small intestine by dietary zinc supplementation. Gut *54*, 469–478.

Davis, D.E., Roh, H.C., Deshmukh, K., Bruinsma, J.J., Schneider, D.L., Guthrie, J., Robertson, J.D., and Kornfeld, K. (2009). The cation diffusion facilitator gene cdf-2 mediates zinc metabolism in Caenorhabditis elegans. Genetics *182*, 1015–1033.

Docampo, R., de Souza, W., Miranda, K., Rohloff, P., and Moreno, S.N. (2005). Acidocalcisomes - conserved from bacteria to man. Nat. Rev. Microbiol. *3*, 251–261.

Eide, D.J. (2006). Zinc transporters and the cellular trafficking of zinc. Biochim. Biophys. Acta *1763*, 711–722.

Eide, D.J. (2009). Homeostatic and adaptive responses to zinc deficiency in Saccharomyces cerevisiae. J. Biol. Chem. *284*, 18565–18569.

Emmert, J.L., and Baker, D.H. (1995). Zinc stores in chickens delay the onset of zinc deficiency symptoms. Poult. Sci. *74*, 1011–1021.

Falcón-Pérez, J.M., and Dell'Angelica, E.C. (2007). Zinc transporter 2 (SLC30A2) can suppress the vesicular zinc defect of adaptor protein 3-depleted fibroblasts by promoting zinc accumulation in lysosomes. Exp. Cell Res. *313*, 1473–1483.

Feeney, G.P., Zheng, D., Kille, P., and Hogstrand, C. (2005). The phylogeny of teleost ZIP and ZnT zinc transporters and their tissue specific expression and response to zinc in zebrafish. Biochim. Biophys. Acta *1732*, 88–95.

Fosmire, G.J. (1990). Zinc toxicity. Am. J. Clin. Nutr. *51*, 225–227.

Gee, K.R., Zhou, Z.L., Ton-That, D., Sensi, S.L., and Weiss, J.H. (2002). Measuring zinc in living cells. A new generation of sensitive and selective fluorescent probes. Cell Calcium *31*, 245–251.

Gourley, B.L., Parker, S.B., Jones, B.J., Zumbrennen, K.B., and Leibold, E.A. (2003). Cytosolic aconitase and ferritin are regulated by iron in Caenorhabditis elegans. J. Biol. Chem. *278*, 3227–3234.

Guo, L., Lichten, L.A., Ryu, M.S., Liuzzi, J.P., Wang, F., and Cousins, R.J. (2010). STAT5-glucocorticoid receptor interaction and MTF-1 regulate the expression of ZnT2 (Slc30a2) in pancreatic acinar cells. Proc. Natl. Acad. Sci. USA *107*, 2818–2823.

Haase, H., and Beyersmann, D. (1999). Uptake and intracellular distribution of labile and total Zn(II) in C6 rat glioma cells investigated with fluorescent probes and atomic absorption. Biometals *12*, 247–254.

Hambidge, M. (2000). Human zinc deficiency. J. Nutr. ***130*** (5S, Suppl), 1344S–1349S.

Hermann, G.J., Schroeder, L.K., Hieb, C.A., Kershner, A.M., Rabbitts, B.M., Fonarev, P., Grant, B.D., and Priess, J.R. (2005). Genetic analysis of lysosomal trafficking in Caenorhabditis elegans. Mol. Biol. Cell *16*, 3273–3288.

Karageorgos, L.E., Isaac, E.L., Brooks, D.A., Ravenscroft, E.M., Davey, R., Hopwood, J.J., and Meikle, P.J. (1997). Lysosomal biogenesis in lysosomal storage disorders. Exp. Cell Res. *234*, 85–97.

Kelly, P., Feakins, R., Domizio, P., Murphy, J., Bevins, C., Wilson, J., McPhail, G., Poulsom, R., and Dhaliwal, W. (2004). Paneth cell granule depletion in the human small intestine under infective and nutritional stress. Clin. Exp. Immunol. *135*, 303–309.

King, J.C. (2011). Zinc: an essential but elusive nutrient. Am. J. Clin. Nutr. *94*, 679S–684S.

Kostich, M., Fire, A., and Fambrough, D.M. (2000). Identification and molecular-genetic characterization of a LAMP/CD68-like protein from Caenorhabditis elegans. J. Cell Sci. *113*, 2595–2606.

Leis, O., Madrid, J.F., Ballesta, J., and Hernández, F. (1997). N- and O-linked oligosaccharides in the secretory granules of rat Paneth cells: an ultrastructural cytochemical study. J. Histochem. Cytochem. *45*, 285–293.

Liao, V.H., and Freedman, J.H. (1998). Cadmium-regulated genes from the nematode Caenorhabditis elegans. Identification and cloning of new

cadmium-responsive genes by differential display. J. Biol. Chem. *273*, 31962–31970.

Lichten, L.A., and Cousins, R.J. (2009). Mammalian zinc transporters: nutritional and physiologic regulation. Annu. Rev. Nutr. *29*, 153–176.

Liuzzi, J.P., Blanchard, R.K., and Cousins, R.J. (2001). Differential regulation of zinc transporter 1, 2, and 4 mRNA expression by dietary zinc in rats. J. Nutr. *131*, 46–52.

MacDiarmid, C.W., Gaither, L.A., and Eide, D. (2000). Zinc transporters that regulate vacuolar zinc storage in *Saccharomyces cerevisiae*. EMBO J. *19*, 2845–2855.

Murakami, M., and Hirano, T. (2008). Intracellular zinc homeostasis and zinc signaling. Cancer Sci. *99*, 1515–1522.

Murphy, J.T., Bruinsma, J.J., Schneider, D.L., Collier, S., Guthrie, J., Chinwalla, A., Robertson, J.D., Mardis, E.R., and Kornfeld, K. (2011). Histidine protects against zinc and nickel toxicity in Caenorhabditis elegans. PLoS Genet. *7*, e1002013.

Palmiter, R.D., Cole, T.B., and Findley, S.D. (1996). ZnT-2, a mammalian protein that confers resistance to zinc by facilitating vesicular sequestration. EMBO J. *15*, 1784–1791.

Praitis, V., Casey, E., Collar, D., and Austin, J. (2001). Creation of low-copy integrated transgenic lines in *Caenorhabditis elegans*. Genetics *157*, 1217–1226.

Rabbitts, B.M., Ciotti, M.K., Miller, N.E., Kramer, M., Lawrenson, A.L., Levitte, S., Kremer, S., Kwan, E., Weis, A.M., and Hermann, G.J. (2008). glo-3, a novel Caenorhabditis elegans gene, is required for lysosome-related organelle biogenesis. Genetics *180*, 857–871.

Rajagopal, A., Rao, A.U., Amigo, J., Tian, M., Upadhyay, S.K., Hall, C., Uhm, S., Mathew, M.K., Fleming, M.D., Paw, B.H., et al. (2008). Haem homeostasis is regulated by the conserved and concerted functions of HRG-1 proteins. Nature *453*, 1127–1131.

Sardiello, M., Palmieri, M., di Ronza, A., Medina, D.L., Valenza, M., Gennarino, V.A., Di Malta, C., Donaudy, F., Embrione, V., Polishchuk, R.S., et al. (2009). A gene network regulating lysosomal biogenesis and function. Science *325*, 473–477.

Schroeder, L.K., Kremer, S., Kramer, M.J., Currie, E., Kwan, E., Watts, J.L., Lawrenson, A.L., and Hermann, G.J. (2007). Function of the Caenorhabditis elegans ABC transporter PGP-2 in the biogenesis of a lysosome-related fat storage organelle. Mol. Biol. Cell *18*, 995–1008.

Simm, C., Lahner, B., Salt, D., LeFurgey, A., Ingram, P., Yandell, B., and Eide, D.J. (2007). Saccharomyces cerevisiae vacuole in zinc storage and intracellular zinc distribution. Eukaryot. Cell *6*, 1166–1177.

Treusch, S., Knuth, S., Slaugenhaupt, S.A., Goldin, E., Grant, B.D., and Fares, H. (2004). Caenorhabditis elegans functional orthologue of human protein h-mucolipin-1 is required for lysosome biogenesis. Proc. Natl. Acad. Sci. USA *101*, 4483–4488.

Vallee, B.L., and Falchuk, K.H. (1993). The biochemical basis of zinc physiology. Physiol. Rev. *73*, 79–118.

Vatamaniuk, O.K., Bucher, E.A., Ward, J.T., and Rea, P.A. (2001). A new pathway for heavy metal detoxification in animals. Phytochelatin synthase is required for cadmium tolerance in Caenorhabditis elegans. J. Biol. Chem. *276*, 20817–20820.

Yoder, J.H., Chong, H., Guan, K.L., and Han, M. (2004). Modulation of KSR activity in *Caenorhabditis elegans* by Zn ions, PAR-1 kinase and PP2A phosphatase. EMBO J. *23*, 111–119.

Zhang, Y., Grant, B., and Hirsh, D. (2001). RME-8, a conserved J-domain protein, is required for endocytosis in Caenorhabditis elegans. Mol. Biol. Cell *12*, 2011–2021.